Poly(thiophenes) functionalised with thiazole heterocycles as electroluminescent polymers

Sarangapani Radhakrishnan and Narayanasastri Somanathan*

Design, synthesis and characterization have been carried out on poly(thiophene)s bearing electron-deficient side chains. The influence of structure on the optical characteristics was studied in detail using molecular orbital calculations. The model compounds have been synthesized and their photoabsorption, photo- and electro-emission characteristics were studied. The results indicate that substituting appropriate heteroaromatic groups to the thiophene chain can enhance electro-emission, even with a single emissive layer, in PLEDs.

Introduction

Conjugated polymers have attracted much attention in recent times due to their potential use in next-generation electronic and optical devices.[1,2] Polymers of this class, with their spatially extended π-bonding systems, offer unique physical properties, unobtainable in conventional polymers. Poly(thiophene)s constitute an important class of conjugated polymers that form some of the most environmentally- and thermally-stable materials which can be used as electrical conductors, nonlinear optical devices, polymeric light emitting diodes (PLEDs), *etc*.[3] The use of poly(thiophene)s in electroluminescent devices has increased enormously as it has high chemical variability, through substitution at the 3 and 4 positions. Poly(3-substituted thiophene)s with a variety of substituents such as alkyl, alkoxy and alkyl heteroatom functionalized side chains have been extensively investigated.[4] In LEDs, to achieve high efficiency, multilayer technology is currently being adopted, where materials containing π-electron deficient heterocyclic moieties have been utilized as an electron-transporting hole-blocking layer (ETHB).[5] These additional layers, however, may cause inhomogeneity in the device due to phase separation/crystallization, which in turn will affect efficiency. This necessitates the designing of ETHB-incorporated single-layer devices. The potential candidates for ETHB function are the nitrogen/oxygen-containing π-electron deficient heterocyclic moieties such as oxadiazoles, triazoles, triazines, pyridines, pyrimidines, quinolines, quinoxalines and extended benzo derivatives, *etc*.[6–9] Hence, the present study focuses on the structure–property relationships of novel poly(thiophene) based materials substituted with 5-membered/6-membered rings containing sulfur and nitrogen at different positions.

The recent growth of computer technologies and the development of quantum chemical program packages make it possible to calculate molecular properties to high precision. However, such a high level of calculation (including electron correlation with a large basis set) for a polymeric system is still restricted to a small unit system in practice.[10] For relatively large systems,[11–14] polymeric structures have been obtained either from the calculations on oligomeric structures or from the experimental measurements. It is well known that Hartree–Fock (HF) level calculations greatly overestimate the HOMO–LUMO gap of a conjugated polymer, due to the inherent problem of the HF theory with unoccupied orbital energy levels.[15] On the other hand, the inclusion of electron correlations leads to a significant underestimation of the gap.[11] Therefore, it is essential to perform numerical experiments that can estimate how much electron correlation should be included to reproduce the experimentally observed HOMO–LUMO gap.[12]

In this regard, well-defined semi-empirical methods are still attractive for a larger or an unknown polymeric system. Quantum-mechanical calculations prove to be extremely useful when dealing with π-conjugated oligomers and polymers.[16] Geometries are usually obtained at semi-empirical levels such as MNDO or AM1.[17] Efficient implementation of density functional theory (DFT) at the local spin density approximation (LSDA) level into solid-state programs[18–20] in recent times has allowed the inclusion of some correlation effects at the *ab initio* level. At the LSDA level, geometries have been shown to improve over those obtained with semi-empirical methods[21] and artifacts were eliminated. However, HOMO–LUMO separations are severely underestimated. It was shown by Salzner *et al*.[22] that by using DFT/hybrid functional calculations, more overlapping with experimental HOMO–LUMO separation could be obtained than with LSDA. Hong *et al*.[23] employed the solid-state version of the MNDO method with the AM1 Hamiltonian to optimize geometrical parameters and to investigate the confirmation behavior of poly(*m*-phenylene) and the related polymer. Born–von Karman periodic boundary conditions and Bloch functions were adopted for crystal calculations. Similar methodology was used to analyze the electronic properties of poly(pentafulvalene), poly(fluorene) and the poly(phenylenevinylene) copolymers.[24,25]

Heterocyclic conjugated polymers[25] such as poly(thiophene) are non-degenerate in the ground state and therefore, two isomers are possible: the aromatic and the quinonoid isomer form, with differing electronic structures. In general, it has

Polymer Laboratory, Central Leather Research Institute, Adyar, Chennai 600 020

been recognized that more stable an isomer, the larger is its HOMO–LUMO separation.[26–28]

The DFT method has been successfully used to study HOMO–LUMO separation in conjugated organic polymers, which also provides a good estimate of the excitation energy.[29–33] Salzner et al.[12] combined the improved geometries of the DFT approach with the improved HOMO–LUMO separation from hybrid functional calculations. HOMO–LUMO separation, ionization potential, electron affinity and bandwidth of the polyheteroaromatics like poly(thiophene), poly(pyrrole) and poly(thiazole) have been estimated using hybrid functional calculations to a greater correlation with the experimentally obtained data. Plotting the results from oligomer calculations against the inverse chain length and extrapolating to infinity obtains the HOMO–LUMO separation for polymers. This approach is well-established for HOMO–LUMO separations and ionization potentials.[34–37] Thus, HOMO–LUMO separation in poly(thiophene) and the related polymers have been computed using DFT methods in this study. Geometries of oligomers have been optimized under the constraint of symmetry at the semi-empirical AM1 level[38] and B3LYP/6-31G* level[39] in density functional theory. The AM1 method is known to produce acceptable conformational behavior for a variety of conjugated molecules[25] in comparison to ab initio and experimental data, although this method yields low rotational barriers.[40] HOMO–LUMO separation of the poly(3-thiophene)-containing heteroaromatic side chains was studied using AM1 and B3LYP/2-31G* or 6-31G*.[41]

The present study aims to explore the structure–property relationships of the novel poly(thiophene) compounds bearing sulfur and nitrogen atoms in the side chains, for light emitting diode applications. The chemical structures of the compounds are shown in Fig. 1. The synthesis of some of the model compounds from the above structures (Fig. 1) has been attempted. The HOMO–LUMO separations of the oligomers of the above structures are calculated using molecular orbital calculations (structures optimized with AM1 and DFT (B3LYP-6-31G*/ZINDO) and the results are compared with the experimental values obtained from absorption spectroscopy. Influence of substituent on the absorption and emission characteristics has been explored qualitatively. The above model compounds are tested for their simulated end-use applications in PLEDs. Among the chemical structures shown in Fig. 1, compounds 2, 3, 4, 5, 6, 8 and 9 were chosen as model compounds for synthesis.

Results and discussion

Recent studies have proved that remarkable luminescence, comparable to that obtained from inorganic or organic materials like PPV etc., can be obtained with 3-subsituted thiophenes.[42] As the color of the emitted light depends on the HOMO–LUMO separation of the π–π* transition, modifications of the above by altering the polymer structure will affect the HOMO–LUMO separation and consequently the emitted color.

Prediction of HOMO–LUMO separation

The interactions between substituents grafted on adjacent monomer units can produce deviation from co-planarity,
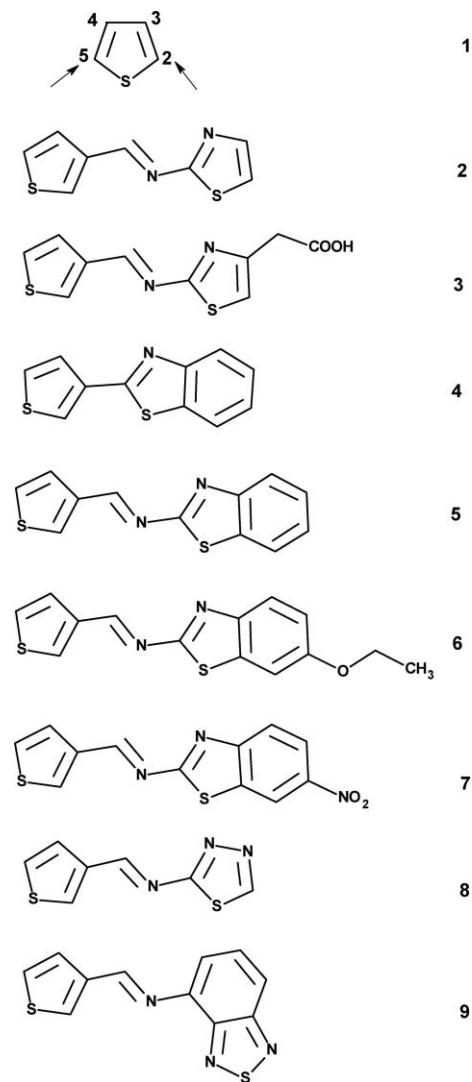

Fig. 1 Different structures of thiophenes (the arrows marked in 1 show the site of polymerization in the thiophene ring).

which depends on both the size of the substituents and their distance from the linking site. The variation in dihedral angle will thus drastically limit the π-electron delocalization along the polymer chain causing a partial loss of its relevant electronic properties.[43] While analyzing the HOMO–LUMO separation obtained from B3LYP/6-31G* for the monomers (Table 1), monomer 4 shows a high value (4.50 eV) and 8 takes the low value of 3.65 eV. This may be attributed to the high extent of conjugation in the case of 8. It can be found from Fig. 1 that compounds 4, 5, 6 and 7 have benzothiazole as a side chain. In 5, 6 and 7, the heteroaromatic ring is connected to thiophene through a –CH=N linkage. At the monomer level, additional π-conjugation may show lowering of energy compared to that of 4. But the observed red shift (Table 1) in 6 and 7, compared to that of 5, is due to the substituent group attached to the benzothiazole group viz. –NO₂ in 7 and –OC₂H₅ in 6. Alkyl substitution affects the absorption spectra in thin films by its influence on the co-planarity of the molecules. Similarly, directly-attached electron donating or accepting groups have a much higher influence compared to

Table 1 HOMO–LUMO separation (eV) of various compounds calculated from B3LYP/6-31G*

Compound		HOMO–LUMO separation	Compound		HOMO–LUMO separation	Compound		HOMO–LUMO separation
1	M	6.391	**4**	M	4.498	**7**	M	4.133
	D	4.399		D	4.337		D	3.612
	T	3.617		T	4.210		T	3.438
	TT	3.214		TT	4.133		TT	3.137
	P	2.225		P	4.055		P	2.950
2	M	3.919	**5**	M	4.251	**8**	M	3.647
	D	3.679		D	3.814		D	3.282
	T	3.561		T	3.711		T	3.248
	TT	3.408		TT	3.438		TT	3.082
	P	3.319		P	3.297		P	2.955
3	M	3.856	**6**	M	3.885	**9**	M	3.982
	D	3.620		D	3.588		D	3.567
	T	3.545		T	3.353		T	3.667
	TT	3.230		TT	3.068		TT	3.608
	P	3.206		P	2.972		P	3.447

a M: monomer; D: dimer; T: trimer; TT: tetramer; P: polymer

simple alkyl substituents. The arrangement of the monomer units in substituted poly(thiophene)s, especially with bulky substituents, can modify their conformational (regio-regularity) features, which in turn, govern the degree of π–π conjugation between adjacent rings.[44,45] For example, ethoxy groups lead to an asymmetric destabilization of the LUMO and HOMO levels of the polymer backbone and the HOMO level being more elevated.[46] On the other hand, electron-withdrawing groups like cyano- or nitro-substitution induces an asymmetric and stronger stabilization of the frontier molecular orbital levels, the LUMO level being more depressed.[47–50]

In monomer **3**, the presence of –COOH reduces the HOMO–LUMO separation compared to monomer **2**. Even though both the monomers of **4** and **5** have same the benzothiazole unit, in **5** it is linked to the thiophene ring through a –CH=N linkage. Even though the monomers of **9** and **8** basically bear a thiadiazole group, **8** shows a reduction in absorption energy of HOMO–LUMO separation compared to **9**, which is due to the variation in linkage. Both **6** and **7** show a red shift from the HOMO–LUMO separation of monomer **5**. This indicates the influence of the –OC$_2$H$_5$ and –NO$_2$ groups on HOMO–LUMO separation. Similarly, due to the influence of –CH$_2$COOH group, the HOMO–LUMO separation energy of **3** is lowered, compared to monomer **2**.

In absorption spectra, major blue shifts of the absorption peaks occur if large differences in the torsional angle between different rings are induced by the substituents. As long as the co-planarity is not distorted, absorption spectra are observed that are similar to unsubstituted oligothiophenes.[51,52]

The calculated HOMO–LUMO separation for the polymer of **4** has a high value of 4.06 eV, whereas both the polymers of **7** and **8** were found to have the lowest value of 2.95 eV. Polymers follow a different trend in HOMO–LUMO separation, as shown in Table 1. The magnitude of HOMO–LUMO separation decreases from monomer to polymer as the chain length increases. Compared to other structures, the polymer of **4** continued to show high HOMO–LUMO separation. It has been reported that the dihedral angle and, thus, the π-orbital overlap between adjacent thiophene rings along the polymer backbone, determine the effective conjugation length along the

polymer chain.[4] In the polymer of **4**, the substituent benzothiazole may impose more steric hindrance to the main chain and lead to the large dihedral angle between the rings and short conjugation along the polymer backbone, resulting in higher blue shifted HOMO–LUMO separation.

Table 2 Wavelength of absorption maxima for monomers and polymers

	Monomer λ/nm	E^{a,b}	Polymer λ/nm	E^{a,b}		Monomer λ/nm	E^{a,b}	Polymer λ/nm	E^{a,b}
2	241	589	245	140	**6**	263	1590	264	135
	272	847	265	104		271	1725	270	155
	338	114	274	95		279	1470	279	107
			283	86		312	400		
			295	76		369	705		
			330	54					
			407	12	**8**	247	284	260	109
3	240	847	235	234		305	91	297	302
	269	899	242	238		313	89	307	213
	355	125	269	242		416	42	332	21
	365	113	288	155				343	19
			314	51				378	14
			323	42	**9**	232	256	224	100
			336	34		250	347	232	87
			351	27		254	337	249	61
			364	22		262	280	262	48
						275	164	293	37
4	248	303	256	210		289	101	300	35
	258	287	263	223		311	65	309	32
	272	354	270	202		322	57		
	280	435	279	152		350	41		
	300	528	292	88		371	29		
	312	481	303	74		395	20		
	327	261	315	64		417	12		
			330	56					
			361	45					
			375	41					
5	264	2500	265	175					
	270	2460	270	200					
	279	1720	278	155					
	293	690							
	346	740							

a E = absorbance of a 1% solution of the substance in a 1.0 cm cell.
b Relationship between E and molar extinction co-efficient $10\varepsilon = E \times$ mol. wt.

Roncali et al.[53] have reported that the steric hindrance of the branched alkyl chain on the polymerization behavior is reduced when the thiophene ring is separated from the branched side chain with more than two carbon atoms. Even though both have benzothiazole side chains, the presence of a –CH=N link may decrease the strain in **5** polymer and hence the low HOMO–LUMO separation. The poorer agreement with experimental data in polymer **6** could be due to the effect of the alkoxy substituent. First, the alkoxy substituent could cause the oligomers to become nonplanar, which would reduce the conjugation.[54] The hydrocarbon segment might promote head-to-head aggregation, which would increase the HOMO–LUMO separation.[55]

Comparison of experimental and theoretical HOMO–LUMO separation

The HOMO–LUMO separation of the molecules is generally determined from the optical absorption threshold.[56] The absorption edge determined from UV-visible spectra in methanol solution is correlated with theoretically obtained HOMO–LUMO separation values (B3LYP/6-31G*). The overlapping absorption edge value obtained from theory and experiment is taken for comparison. Comparisons of the predicted HOMO–LUMO separation with the experimental results are shown in Fig. 2. Monomers **4** and **8** show high and low HOMO–LUMO separation both in solution and in thin films. In general, the HOMO–LUMO separation obtained from experimental data follows the same trend of B3LYP/6-31G* calculated values. The monomer of **9** has a good overlap of HOMO–LUMO separation with theory, while polymer **9** shows more deviation from the experimentally determined value in solution. Experimental HOMO–LUMO separation data of monomers show more overlap with their corresponding theoretical value than their corresponding polymers. The absorption edge is also determined for thin films (prepared from CHCl₃ solution) and compared with theoretically-obtained HOMO–LUMO separation (B3LYP/6-31G*). The variation between the HOMO–LUMO separation, calculated from solution and thin film data also match well, unlike in their corresponding polymers. In general, the HOMO–LUMO separation values obtained for thin films are lower than the values obtained for solution. Kwon and McKee[54] reported that the smaller HOMO–LUMO separation in thin films is due to the more planar conformation of the oligomers in the solid state.

The polymers of compounds containing thiazole (**2**) and thiadiazole (**9**) at the terminal point of the side chain show more deviation from the experimental values. The deviation between experimental and calculated HOMO–LUMO separation values is observed to be high in the case of compounds which have terminal functional groups in the side chain (which again influence the solvatochromism/aggregate formation), as in the case of **3** and **6**. This is more pronounced in **3**, where the presence of terminal carboxylic acid may play a role in the deviation. On the other hand, polymers containing fused phenyl rings in the side chain (like in **4** and **5**) show significant overlap in the theoretical and experimental values.
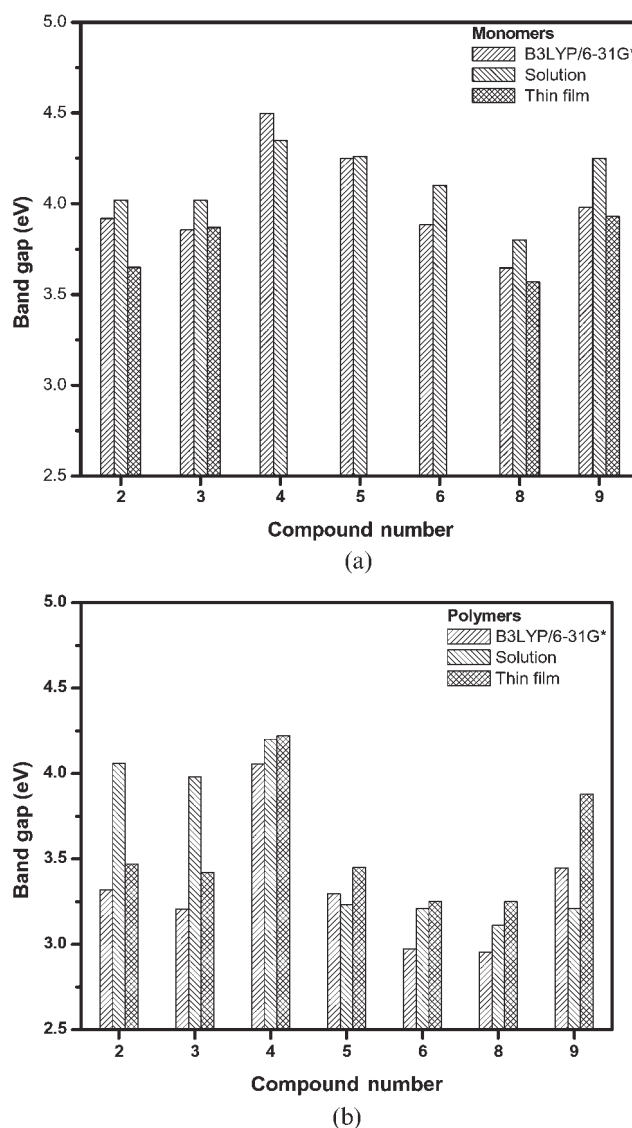
Fig. 2 Comparison of HOMO–LUMO separation values obtained by theory and experiment; (a) monomers; (b) polymers.

Although the HOMO–LUMO separation shows little deviation from the experimentally-obtained HOMO–LUMO separation, the trend in HOMO–LUMO separation is found in most cases to be the same in the experimental and theoretical results. The possible reasons for the deviation in results may be (i) the gas phase is considered in the theoretical calculation; (ii) only HT–HT coupling is considered in the theoretical calculations,[57] but in real cases, the polymer may have regio-random configurations; (iii) intermolecular interactions are not considered in the calculations.

Prediction of absorption maxima and comparison with experimental results

The absorption maxima of organic compounds can be predicted by the semi-empirical molecular orbital calculations (ZINDO for electronic transition energies).[55,58] The peak values of the experimentally-obtained absorption spectra (solution and thin film) of monomers and polymers are

determined from the second derivative of the experimentally-determined spectra. The predicted transitions from ZINDO calculations are compared with the experimentally obtained absorption maximum.

In Fig. 3, theoretically predicted (with ZINDO) wavelength maxima with maximum oscillator strength and experimental λ_{max}, obtained in the same range (both solution and thin film) of monomers and polymers are compared. The predicted and experimentally-observed absorption maximum is ordered by decreasing energy. In monomers, both solution and thin film data follow the same trend as the theoretical data. The λ_{max}, obtained from polymer thin films, slightly deviates from experimental data. Thin film λ_{max} of polymer **3** shows deviation from the theoretical trend, which may be due to the influence of solid-state packing, as mentioned earlier. In the case of polymer solutions, the predicted trend is in agreement with the experimentally observed trend.

The deviation in the trend of ZINDO results of polymer thin films can be attributed to the interactions involved in the

Fig. 4 Photoabsorption spectra obtained for different monomer solutions in methanol.

polymeric chains. In general, the ZINDO-predicted λ_{max} is in agreement with experimental data. Slight deviation in some cases can be attributed to parameterization of ZINDO. ZINDO was parameterized on small molecules and not in general on oligomers of large size. The effectiveness of computational method, will be determined both by the accuracy of the resulting transition energies and by the accuracy of the predicted oscillator strengths.[59]

Influence of chemical structures on photoabsorption, fluorescence (photoluminescence [PL]) and electro luminescence (EL) characteristics

Photoabsorption

The absorption spectra obtained for different monomers and polymers are presented in Fig. 4 and 5, respectively. The different wavelengths of absorption maxima obtained for
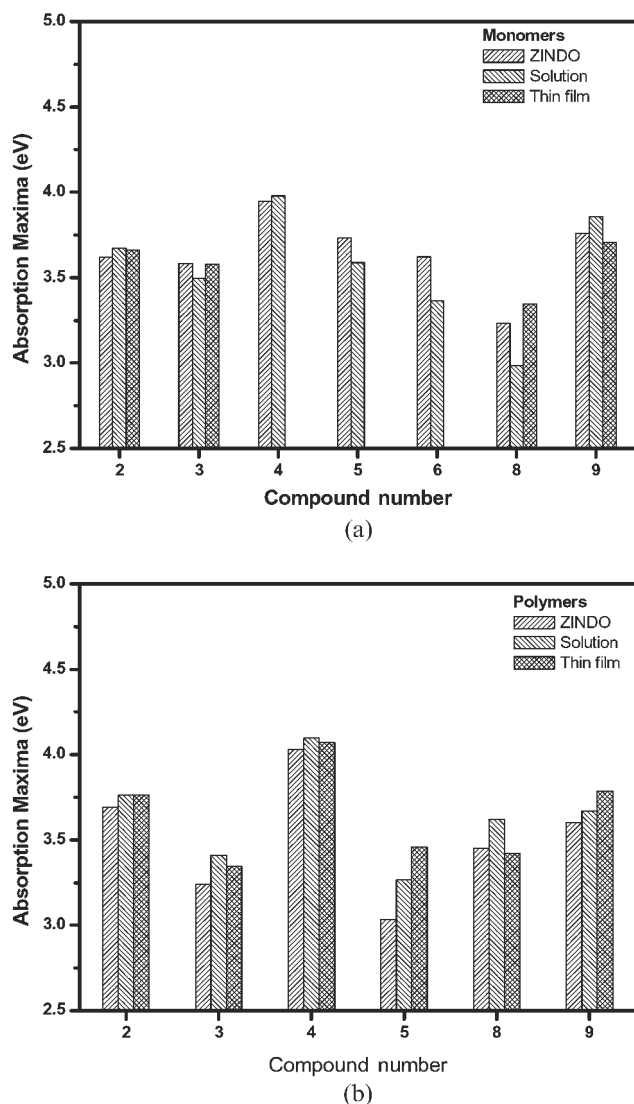

(a)

(b)

Fig. 3 Comparison of absorption maxima obtained by ZINDO and experiments; (a) monomers; (b) polymers.
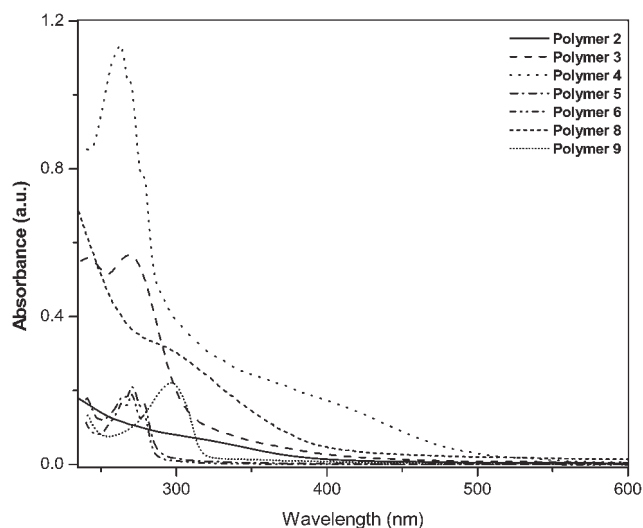
Fig. 5 Photoabsorption spectra obtained for different polymer solutions in methanol.

Table 3 Photoluminescence wavelengths of monomers and polymers in methanol

Monomer	λ_{exc}	Wavelengths of emission (normalized intensity value)/nm
2	272	324 (0.48), 411 (0.56), 515 (1.0), 589 (0.41)
3	268	313 (0.42), 423 (1.0), 584 (0.25), 602 (0.17)
4	258	358 (0.84), 379 (1.0), 430 (0.42), 708 (0.12)
5	264	302 (0.43), 363 (0.51), 380 (0.55), 400 (0.52), 431 (0.39), 565 (1.0), 632 (0.42)
6	271	357 (0.55), 375 (0.74), 403 (1.0), 429 (0.86), 451 (0.51), 518 (0.24)
8	243	295 (0.84), 306 (0.52), 317 (1.0), 527 (0.09), 551 (0.13), 564 (0.17), 583 (0.46), 603 (0.46), 636 (0.32)
9	250	320 (0.58), 380 (0.75), 403 (0.84), 428 (0.94), 468 (1.0), 582 (0.48), 603 (0.44)
Polymer	**λ_{exc}**	**Wavelengths of emission (normalized intensity value)/nm**
2	275	317 (1.0), 432 (0.22), 469 (0.13), 572 (0.67), 583 (0.69), 597 (0.58), 644 (0.22)
3	267	318 (0.58), 373 (1.0), 417 (0.89), 455 (0.63), 583 (0.26), 626 (0.2), 710 (0.09)
4	262	307 (0.09), 357 (0.2), 370 (0.21), 427 (0.33), 471 (0.92), 493 (1.0)
5	265	303 (0.59), 356 (1.0), 555 (0.46), 566 (0.23), 605 (0.37)
6	264	328 (0.70), 346 (1.0), 353 (0.96), 362 (0.92), 468 (0.38), 565 (0.23), 651 (0.20), 688 (0.17)
8	299	332 (1.0)
9	232	313 (0.64), 330 (0.96), 343 (1.0), 422 (0.32), 495 (0.18), 585 (0.21), 610 (0.21), 656 (0.21), 688 (0.15)

different monomers and polymers, respectively, are presented in Table 2. The absorption spectra obtained for different structures are analyzed on the basis of second derivative curves and the maxima are individually compared with similar structures. In order to understand the effectiveness of absorption, the molar extinction coefficient of different absorptions is presented in Table 3. Comparison of data obtained for monomers of **2** and **3** indicate that, due to the influence of CH_2COOH group, the 338 nm absorption is red shifted to 355 nm. Due to the presence of an additional side chain, monomer **3** has more side chain absorptivity than monomer **2**. Due to the presence of $-OC_2H_5$, the 293 and 346 nm absoprtions are shifted to 312 and 369 nm, respectively (in monomer **6** compared with monomer **5**). The absorption values in polymer of **3** are red shifted due to the influence of the additional CH_2COOH group. Unlike the monomers, there is no characteristic variation in absorption between polymer **5** and **6**.

Photoluminescence

In order to compare all the emission wavelengths obtained from the different compounds, the compounds are excited with wavelengths where the co-efficient of absorption was found to be very high. The representative PL spectra obtained for **2**, **4** and **6** are presented in Fig. 6. [Fig. 6a shows the expanded overlap of the peaks of the monomers, since the obtained PL intensity values of the monomers shows tremendous variation (*y*-axis not to scale), while Fig. 6b is made to scale]. Similarly the PL spectra obtained for representative polymers **3**, **5** and **8** are presented in Fig. 7 (*y*-axis not to scale) to show the influence of structure on the PL wavelengths.

The intensity values at different wavelengths of PL are related to the probability of PL and are therefore taken for comparison, to understand the influence of structure (functional groups, linkages, *etc.*) on PL. A normalization procedure has been adopted to compare qualitatively the fluorescence of different compounds. The maximum emission intensity obtained from a compound is taken as 100% and the intensities obtained at other wavelengths in the PL spectra are

(a)

(b)
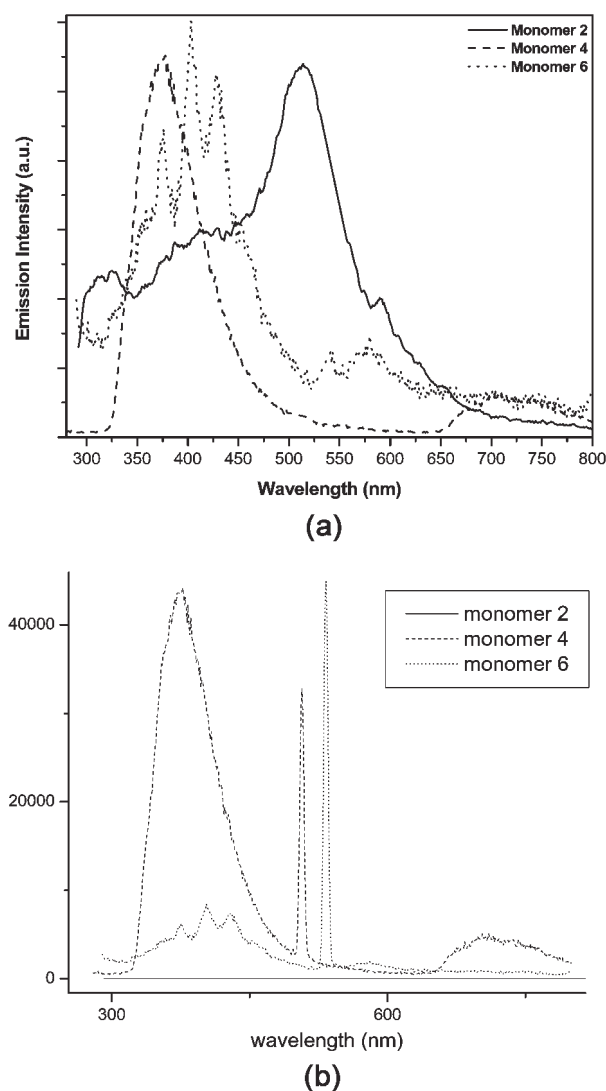
Fig. 6 PL spectra (solution) of monomers **2**, **4** and **6**; (a) spectra showing the wavelengths for comparison (*y*-axis not to scale); (b) original PL spectra (to scale); peaks with very narrow band width are doublet peaks.
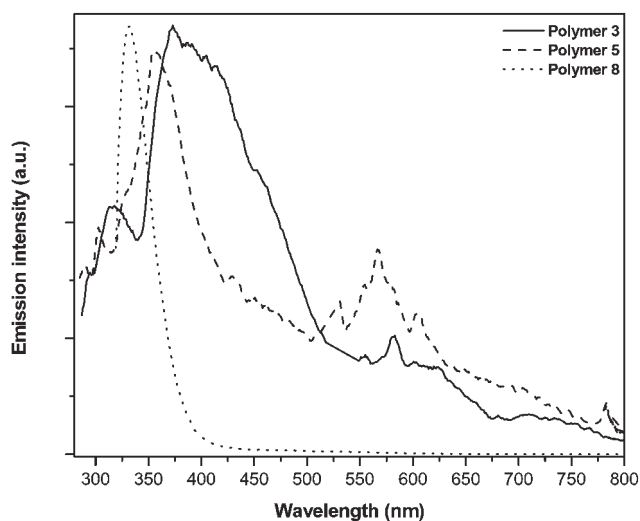
Fig. 7 PL spectra (solution) of polymers **3**, **5** and **8** (*y*-axis not to scale).

normalized with reference to the above. The corresponding normalized values at different intensities for various structures (solution) are presented in Table 3. The normalized intensity fraction of that compound is given in parentheses. Experiments were performed with methanol solutions of all compounds of the same concentration and the variation in properties can be attributed to the influence of structure. Similarly, the thin films for fluorescence experiments of all compounds are prepared from chloroform solution. In general, the emission is obtained in all base color ranges (blue, green and red) apart from the UV range. On the basis of normalized emission intensities in different wavelength regions, the prominent wavelength range of emission is fixed and the compounds are graded on the basis of descending energy (considering the energy/wavelength and the intensity at that wavelength). In the case of, *e.g.*, the compound emitting more intensity in UV/blue wavelength region and very low intensity in the green region, it is considered to take a higher position in the emission-ordering of compounds. Monomer **6**, which emits at high intensity (44065 a.u., shown in Fig. 6) in the UV region (very high intensity and very high energy) is graded the highest, while monomer **2**, the intense emission of which falls at 515 nm (a very low intensity (5.4 a.u.) compared to monomer **6**, and a very low energy region) is considered the

lowest in the monomer order. The procedure was adopted for monomers and polymers to understand the influence of structure on PL.

The qualitative comparison of the PL order of the monomers taken for study areas was as follows: **4 > 8 > 9 > 6 > 5 > 3 > 2**. The PL ordering of the polymers (in methanol) is given as follows: **8 > 4 > 9 > 3 > 2 > 6 > 5**. Even though the overall HOMO–LUMO separation order is followed in PL too, there are some deviations in the emission trend which can be attributed to the presence of solvation and its influence over different structures containing various functional groups. It is interesting to note that the structures under study show binding on the wavelength of the PL studied in solution. In the case of, *e.g.*, the polymers of **2** and **3**, which have comparable structures, these show variation in emission wavelength. The peaks at 432 and 469 nm of polymer **2** are shifted to 417 and 455 nm in polymer **3**, respectively. In the case of polymer **5**, the 356 nm peak is shifted to 346 nm in polymer **6**. The 324 nm peak of monomer **2** is blue shifted to the 313 nm peak obtained for monomer **3**.

The PL is studied for different compounds in thin films prepared from chloroform solution. Even though it is known that aggregation/packing and, therefore, the optical characteristics are influenced by the method of preparation and solvent used, a solvent with less polarity *viz.* chloroform is used, since it gave good thin films. The qualitative comparison of thin film PL for the compounds was conducted by adopting the procedure mentioned earlier and the obtained results are presented in Table 4. The optical grade thin film could not be obtained for monomers **4**, **5** and **6**. The trends obtained for thin films of the compounds of different groups are presented below.

Monomer: **9 > 2 > 3 > 8**
Polymer: **8 > 5 > 6 > 4 > 9 > 2**

The trends obtained in thin film photoemission of different compounds show variation in values to those of solution based PL. For solution studies, methanol is used, while for thin film preparation chloroform is used. The polarity of the solvent and its corresponding interactions with the functional groups/aggregation may possibly be the reason for this modification. The emission wavelengths of solution and thin film indicate the influence of packing as well as solvatochromism in monomers. The peaks at 315 and 454 nm obtained in thin films of monomer **9** are red shifted to 380 and 468 nm, respectively, in solution due to the above-mentioned influence. Similarly, in

Table 4 Photoluminescence wavelengths of the monomers and polymers in thin film

Monomer	λ_{exc}	Wavelengths of emission (normalized intensity value)/nm
2	244	323 (0.97), 430 (1.0), 608 (0.47)
3	246	322 (0.45), 361 (0.45), 399 (0.63), 532 (1.0)
8	262	305 (1.0), 350 (0.7), 456 (0.83), 604 (0.63)
9	253	315 (1.0), 436 (0.88), 454 (1.0), 630 (0.39)
Polymer	λ_{exc}	**Wavelengths of emission (normalized intensity value)/nm**
2	230	311 (0.57), 366 (0.58), 531 (1.0), 556 (0.86), 567 (0.89), 612 (0.37)
3	237	311 (1.0)
4	245	316 (1.0), 594 (0.86)
5	224	277 (0.67), 327 (1.0), 428 (0.84), 480 (0.52), 534 (0.42), 564 (0.38)
6	226	274 (0.57), 315 (0.96), 324 (1.0), 369 (0.64), 422 (0.76), 431 (0.82), 480 (0.52), 538 (0.46), 564 (0.37)
8	226	274 (0.64), 322 (1.0), 366 (0.63), 436 (0.64), 485 (0.43), 510 (0.28), 533 (0.36), 564 (0.30)
9	231	308 (0.54), 329 (0.52), 367 (0.59), 532 (1.0), 564 (0.87)

Table 5 Total intensity of electroluminescence data obtained for various polymers

Compound	Intensity of emission	Threshold voltage/V
2	3040	2.9
3	4270	3.1
4	2860	4.1
5	3720	3.3
6	2350	3.3
8	1900	3.2
9	4515	3.1

monomer **2**, even though the wavelength of emission obtained in the UV region is not shifted, the 430 nm peak (thin film) is blue shifted to 411 nm.
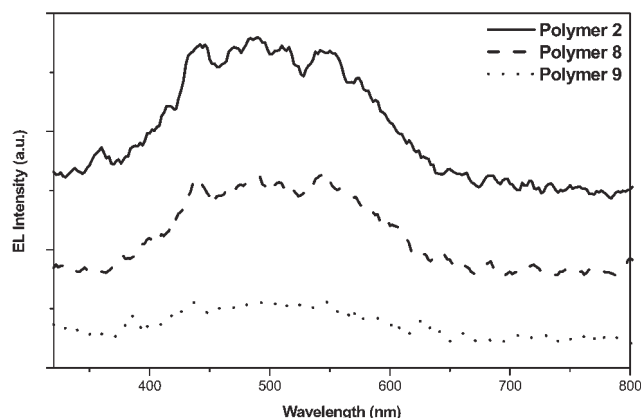
Electroluminescence (EL)

In the present study, the electro-emission of single layer LEDs containing thiophene compounds as the emissive layer is critically analyzed, to understand the influence of structure on EL intensity. The values presented in Table 5 represent the highest intensity values obtained between 0–5 V applied voltages in continuous mode. Indium tin oxide (ITO) and aluminium are used as the anode and cathode for all the devices containing different thiophene compounds.

Polymer **9** shows the highest total EL intensity, while **8** shows the lowest value. The total intensity of emission in polymer **3** is also comparably high. The order of total electroluminescence intensity is as follows:

9 > 3 > 5 > 2 > 4 > 6 > 8

The threshold forward bias voltage (the voltage at which the electro-emission starts from zero) for the compounds are also presented in Table 5. Polymer **4** shows the highest forward bias voltage. The diodes prepared with other polymers show a bias around the same threshold voltage (*ca.* 3 V). The highest threshold voltage of polymer **4** can be explained on the basis of the lowest electron affinity and electronegativity (on the basis of theoretical DFT calculations and HOMO–LUMO data) in contrast to other compounds. Even though the obtained intensity is low in compound **3**, the total emission intensity tremendously increases with the increase of applied voltage. In polymer **3**, the emission intensity continued to increase with the increase of voltage. There is a 9-fold increase at 5.5 V, which increases further to 13 fold at 18 V. The stability of the devices prepared with polymer **3** is high and it continues to give comparable emission intensity even after 10 cycles in air (under unencapsulated conditions).

Many of the other compounds taken for study do not show any characteristic change with increasing voltage. The higher

Fig. 8 Electroluminescence spectra obtained for polymers 2, 8 and 9 (*y*-axis not to scale).

intensity of emission with voltage can be again understood on the basis of high electron affinity and high electronegativity. The overall results suggest that the electron affinity and negativity play a dominant role in enhancing EL intensity (obtained from theoretical calculations). The most widely-used material for electron transporting/hole blocking functionalities is based on the nitrogen-containing five membered hetero-aromatic rings which enhance electron affinity.[60] It is interesting to note that the results obtained from electro-emission intensity with the thiophene compounds under study (Fig. 1) clearly indicate that substitution of appropriate heteroaromatic groups to the thiophene chain can enhance the EL even with single emissive layer in PLEDs.

Since it is our aim to have all base color emissions with single emissive material, the results obtained from single layer LEDs with different polymers were analyzed using a spectro-fluorimeter for wavelengths of EL and their corresponding intensity contribution towards the total emission intensity. The results obtained for various polymers are presented in Table 6. The representative EL obtained for polymers **2**, **8** and **9** are shown in Fig. 8 (*y*-axis not to scale). A normalization procedure similar to photoemission (explained earlier) is followed, in order to understand the relation between the wavelength of electro-emission intensity and structure. The electro-emission in the UV range could only be recorded from 320 nm, due to experimental limitations. This also depends on the applied voltage.

Qualitative ordering of polymers on the basis of EL patterns is obtained from the data shown in Table 6, on the basis of wavelength/intensity. The qualitative ordering of the wavelength of electro-emission overlaps with the results of PL. This

Table 6 Electroluminescence wavelengths of polymers

Polymer	Wavelengths of emission (normalized intensity value)/nm
2	415 (0.55), 443 (0.96), 471 (0.94), 489 (1.0), 510 (0.94), 544 (0.91), 574 (0.74)
3	442 (0.84), 479 (1.0), 506 (1.0), 544 (0.79), 578 (0.49)
4	404 (0.44), 436 (0.93), 480 (0.89), 494 (096), 508 (1.0), 527 (0.85), 548 (0.93), 561 (0.76), 584 (0.65), 615 (0.41)
5	396 (0.42), 420 (0.47), 444 (0.76), 468 (0.84), 480 (0.91), 496 (1.0), 544 (1.0), 586 (0.69), 606 (0.36)
6	442 (0.89), 478 (1.0), 508 (0.92), 550 (0.98), 574 (0.67), 588 (0.56), 608 (0.40)
8	406 (0.37), 440 (0.95), 492 (0.97), 508 (0.92), 546 (1.0), 566 (0.8), 582 (0.6), 598 (0.54)
9	436 (0.97), 470 (0.83), 482 (0.87), 496 (0.93), 518 (0.83), 544 (0.97), 550 (1.0)

suggests that the excited state formation and the emitting species involved in each case may be similar.

In this study, at the applied voltage of 5 V, the EL wavelength was analyzed for all compounds, but the polarity of the compounds varies due to the structural contribution of the functional groups, which change the semiconducting properties and, therefore, the current density. As a result, further studies at constant current density may give a true picture of overlap of PL and EL properties. The electron density of thin films is also influenced by the method of preparation and the solvent used for spin coating, which has to be taken in consideration for further study. The output of electro-emission is also dependent on factors such as charge injection ratios, charge mobility and extra quenching processes due to electrodes and charge carriers. Therefore, within the limited framework of identical conditions, the structures of the emissive layers are correlated with the electro-emission intensity and the results show an overlap of structural influence on the enhancement of electro-emission in a single emissive layer containing a self-sustained electron transporting function.

Summary

The molecular orbital calculations have been performed on oligomers of thiophene-bearing heterocyclic side chains to understand their structure–property relationships. The model compounds have been synthesized and characterized using spectroscopic techniques. Comparison of theoretical HOMO–LUMO separation with the experimentally-obtained absorption edges shows that, in general, the trend in HOMO–LUMO separation is found to be same in both cases. Similar to the HOMO–LUMO separation, the experimental wavelength maxima also correlate well with ZINDO results. The synthesized model polymers were studied for their photo-absorption and PL characteristics. This is useful for understanding the effect of structure on optical characteristics. The polymers were tested for its end-use applications in polymeric light emitting diodes by fabricating single emissive layer PLEDs. The structures of the emissive layers are correlated with the EL intensity and the results show an overlap of structural influence on the enhancement of EL in a single emissive layer containing a self-sustained electron transporting functionality.

Experimental

Synthesis of monomers 2, 3, 5, 6, 8 and 9

The corresponding amine, dissolved in ethanol was reacted with thiophene-3-carboxaldehyde in the presence of a catalytic amount of acetic acid. The mixture was refluxed for 1–6 h and the resulting solid was filtered and washed with ethanol. The compound was purified by recrystallisation.

Monomer 2. IR (cm^{-1}): 3100, 2943, 2857, 1605, 1513, 1447, 1412, 1321, 1148, 1074, 867, 834, 764, 692, 613; ^{1}H NMR (300 MHz, DMSO, ppm): 8.56 (d, 1H), 8.31 (d, 1H), 8.27 (s, 1H), 7.38 (m, 1H) and 7.08 (m, 2H); ^{13}C NMR (75 MHz, DMSO, ppm): 157, 143.2, 139.5, 127.5, 126.9, 122.5, 122.4 and

107.6. Elemental analysis: calculated: C: 49.50%; H: 3.09%; N: 14.43%, S: 32.98%, experimental: C: 48.10%; H: 3.01; N: 15.03; S: 34.86%.

Monomer 3. IR (cm^{-1}): 3099, 2948, 2915, 1604, 1519, 1413, 1376, 1319, 1147, 957, 867, 837, 787, 756, 693, 638; ^{1}H NMR (300 MHz, CDCl$_3$, ppm): 9.92 (s, 1H), 8.81 (s, 1H), 8.08 (s, 1H), 7.35 (m, 1H), 7.18 (m, 2H) and 3.86 (s, 2H); ^{13}C NMR (75 MHz, CDCl$_3$, ppm): 165, 157, 143.8, 143.4, 133, 127.7, 126, 123.7, 122.1, and 36. Elemental analysis: calculated: C: 25.39%; H: 3.17%; N: 11.11%, S: 25.39%, O: 12.69% experimental: C: 47.50%; H: 3.09%; N: 12.13%; S: 27.10%.

Monomer 5. IR (cm^{-1}): 3096, 3062, 2949, 2847, 1602, 1538, 1446, 1412, 1309, 1261, 1218, 1162, 1101, 1016, 936, 884, 840, 789, 749, 691,623, 577, 473 and 430; ^{1}H NMR (300 MHz, DMSO, ppm): 9.14 (s, 1H), {[7.84 (d), 7.76 (s), 7.61 (d), 7.39 (m), 7.18 (t)], 7H}. ^{13}C NMR (75 MHz, DMSO, ppm): 164.60, 161.07, 152.11, 141.08, 130.61, 128.48, 126.67, 125.52, 122.87, 121.29, 120.95, and 118.52. Elemental analysis: calculated: C: 59.01%; H: 3.27%; N: 11.48%; S: 26.22%, experimental: C: 57.04%; H: 3.21%; N: 12.07%; S: 27.72%.

Monomer 6. IR (cm^{-1}): 3083, 2973, 2923, 2857, 1604, 1519, 1449, 1390, 1333, 1261, 1221, 1121, 1051, 943, 905, 869, 821, 795, 710, 681, 645, 586 and 526; ^{1}H NMR (300 MHz, CDCl$_3$, ppm): 8.91 (s, 1H), {[7.96 (s), 7.82 (d), 7.72 (d)], 3H}, {[7.36 (t), 7.21 (d), 7.03 (dd)], 3H}, 4.03 (q, 2H), 1.42 (t, 3H); ^{13}C NMR (75 MHz, CDCl$_3$, ppm): 169.14, 158.32, 156.83, 145.80, 139.42, 135.51, 133.77, 126.97, 126.10, 123.45, 115.84, 104.91, 63.89, and 14.65. Elemental analysis: calculated: C: 58.33%; H: 4.17%; N: 9.72%; S: 22.22%; O: 5.55% experimental: C: 56.80%; H: 3.90%; N: 10.78%; S: 23.45%.

Monomer 8. IR (cm^{-1}): 3098, 1611, 1556, 1497, 1403, 1295, 1262, 886, 836, 773, 743, 615; ^{1}H NMR (300 MHz, DMSO, ppm): 8.57 (s, 1H), 8.30 (s, 1H), 7.39 (m, 1H), 7.16 (m, 2H); ^{13}C NMR (75 MHz, DMSO, ppm): 154.0, 151.7, 138.0, 128.0, 124.5, 122.5, 121.8. Elemental analysis: calculated: C: 43.08%; H: 2.56%; N: 21.53%; S: 32.82%, experimental: C: 43.18%; H: 2.52%; N: 21.40%; S: 32.90%.

Monomer 9. IR (cm^{-1}): 3087, 1607, 1442, 1335, 1198, 1107, 1078, 1022, 945, 892, 848, 783, 665, 609; ^{1}H NMR (300 MHz, CDCl$_3$, ppm) 8.11 (s, 1H), 7.89 (d, 1H), 7.78 (d, 1H), 7.38 (t, 1H), 7.31 (m, 1H) and 7.22 (m, 2H); ^{13}C NMR (75 MHz, CDCl$_3$, ppm): 157.6, 155.9, 155, 148, 143.6, 137.6, 131.3, 129.9, 128.9, 125.6 and 122.7. Elemental analysis: calculated: C: 53.88%; H: 2.85%; N: 17.14%; S: 26.12%, experimental: C: 52.80%; H: 2.76%; N: 17.04%; S: 27.40%.

Synthesis of monomer 4

3-Bromothiophene (0.01 mol) and magnesium turnings (0.01 mol) were introduced together with dry diethyl ether in a three necked flask fitted with a condenser, a dropping funnel and nitrogen inlet. The entrainer, 1, 2-dibromoethane (0.01 mol) in anhydrous diethyl ether, was then added at ice-cold temperature for a period of 8 h. After the setting of the

reaction, the solution was brought to ambient temperature. The resulting Grignard compound was transferred to a second dropping funnel fitted to a second three necked flask containing 2-chlorobenzothiazole (0.01 mol) and 1,3- bis(diphenylphosphinopropane)nickel(II) chloride (Nidppp) in anhydrous diethyl ether. The Grignard compound was added dropwise at 0 °C and the resulting adduct was allowed to warm up to ambient temperature and stirred for 1 h. The contents were refluxed for 24 h. The obtained mixture was neutralized with very dilute aqueous hydrochloric acid. The organic layer was washed with water, dried and concentrated. The crude product was purified on a silica gel column using petroleum ether (boiling range 60–80 °C) as the eluent.

IR (cm^{-1}): 3087, 3057, 1588, 1539, 1477, 1432, 1398, 1373, 1312, 1240, 1184, 1123, 1074, 993, 943, 893, 870, 838, 786, 765, 730, 689, 653, 588 and 436; ^1H NMR (300 MHz, $CDCl_3$, ppm): 8.02 (t,2H); 7.85 (d,1H); 7.69 (d,1H); 7.39 (m,3H); ^{13}C NMR (75 MHz, $CDCl_3$, ppm): 162.6; 153.8; 135.9; 134.6; 126.8; 126.5; 126.2; 126.0; 125.0; 123.0; 121.5. Elemental analysis: calculated: C: 60.82%; H: 3.23%; N: 6.45%; S: 29.49%, experimental: C: 60.20%; H: 3.13%; N: 8.68%; S: 28.99%.

Electrochemical polymerization

The electrochemical polymerization of Schiff's bases was carried out in acetonitrile containing tetrabutylammonium hexafluorophosphate ($TBAPF_6$) as the electrolyte. The current density for the polymerization reaction was 1.43 mA cm^{-2} and the reaction was performed for 4 h with this current density. Then dedoping of the formed polymers was carried out for 30 min by reversing the polarity. The time of reaction and dedoping were fixed on the basis of the applied current. The above general procedure was adopted for the synthesis of all polymers.

Absorption spectra of the samples (both in methanol solution and in thin films) were recorded using Cary UV-50-Bio UV-Visible spectrophotometer. The photoemission spectrum of the sample was studied using a Cary Eclipse fluorescence spectrophotometer. Thin films for the study were prepared by coating the sample solution over quartz plates using spin coating technique coated at 3000 rpm.

Fabrication and analysis of LEDs. Light emitting diodes were fabricated by spin coating the emissive polymer layer over the indium tin oxide (ITO) coated (100-nm thickness) glass plates. The thin film was formed by spin coating the chloroform solution of the polymer at 3000 rpm. Aluminium was coated over the electro-emissive polymer layer using an E306 Edwards coating unit. Aluminium serves as the cathode and ITO acts as the anode in the diode. The total emission intensity of the LEDs was tested as a function of voltage using a luminometer (Nucleonix) containing a photomultiplier tube housing with drawer assembly type PT 168. The LEDs were tested under continuous application of voltage, and the forward bias threshold voltage and total intensity of the emission were obtained. The wavelength of electro-emission was studied using the Cary Eclipse fluorescence spectrophotometer. The LEDs were kept in the solid sample holder in such a way that the ITO side faced the analyzer. Voltage was applied to the diode and the emission wavelength was recorded using a spectrofluorimeter.

Theoretical methodology

The Cerius^2 package from Accelrys was used for generating the initial geometries and the Gaussian 98 program[61] was used for semi-empirical AM1 and density functional calculations (B3LYP/6-31 G*). The geometries of the oligomers were optimized using a semi-empirical AM1 Hamiltonian. Then, DFT (B3LYP/6-31 G*) single point calculations were made for geometries optimized from AM1 calculation. For comparison, the parent thiophene oligomers (T) were also optimized.

These molecular orbital calculations were performed to estimate the HOMO–LUMO separation (EG) and this was calculated by taking the difference between the highest occupied molecular orbital (HOMO) and the lowest unoccupied molecular orbital (LUMO). HOMO–LUMO separation of the polymer is obtained from the HOMO–LUMO separation data of the oligomers by extrapolating to infinite chain length, using an oligomeric approach.[55] The geometry characterizations were extended to measure the torsion angles between the adjacent thiophene rings and other substituents in the side chain.

Photoabsorption maxima of π-conjugated organic molecules can be predicted by ZINDO, which is parameterized explicitly for predicting excitation energies[62]. Hence, semi-empirical ZINDO calculations were performed for AM1 optimized geometries. Due to the limitations of the ZINDO method, structures with a larger size (i.e., a greater number of atoms) of some of trimer and tetramer structures were not possible.[22] Absorption maxima of the polymer were obtained by plotting the excitation energy of monomers, dimers, trimers and tetramers versus the inverse chain length in a similar way to the method mentioned above. The first excited state with significant oscillator strength was considered for extrapolation, to find the value for the polymer. However, in some cases more transitions with comparable oscillator strengths were also used for comparison.

References

1 B. J. Schwartz, *Annu. Rev. Phys. Chem.*, 2003, **54**, 141.
2 A. Kraft, A. C. Grimsdale and A. B. Holmes, *Angew. Chem., Int. Ed.*, 1998, **37**, 402.
3 J. Roncali, *Chem. Rev.*, 1997, **97**, 173.
4 L. Akcelrud, *Prog. Polym. Sci.*, 2003, **28**, 875.
5 M. Thelakkat and H. W. Schmidt, *Polym. Adv. Technol.*, 1998, **9**, 429.
6 S. H. Ahn, M. Czae, E. R. Kim, H. Lee, S. Ho Han, J. Noh and M. Hara, *Macromolecules*, 2001, **34**, 2522.
7 S. H. Ahn, T. K. Ahn, S. H. Han and H. Lee, *Mol. Cryst. Liq. Cryst.*, 2000, **349**, 459.
8 J. H. Promislow, J. Preston and E. T. Samulski, *Macromolecules*, 1993, **26**, 1793.
9 J. Belmar, M. Parra, C. Zuniga, C. Perez, C. Munoz, A. Omenat and J. L. Serrano, *Liq. Cryst.*, 1999, **26**, 389.
10 M. Springborg, *Int. J. Quantum Chem.*, 2000, **77**, 843.
11 U. Salzner, J. B. Lagowski, P. G. Pickup and R. A. J. Poirier, *J. Comput. Chem.*, 1997, **18**, 1943.
12 U. Salzner, P. G. Pickup, R. A. Poinier and J. B. Lagowski, *J. Phys. Chem. A*, 1998, **102**, 2572.
13 M. E. Vaschetto, B. A. Ratamal, A. P. Monkman and M. Springborg, *J. Phys. Chem. A*, 1999, **103**, 11096.

14 S. L. Lim, K. L. Tan, E. T. Kang and W. S. Chin, *J. Chem. Phys.*, 2000, **112**, 10648.
15 W. J. Hunt and A. Goddard, *Chem. Phys. Lett.*, 1969, **3**, 414.
16 J. L. Bredas, *Synth. Met.*, 1997, **84**, 3.
17 M. J. S. Dewar, E. G. Zoebisch, E. F. Healer and J. J. P. Stewart, *J. Am. Chem. Soc.*, 1985, **107**, 3902.
18 G. Brocks, P. J. Kelly and R. Car, *Synth. Met.*, 1993, **55–57**, 4243.
19 I. P. Gomes da Costa, R. G. Dandrea, E. M. Conwell, M. Fahlman, M. Logdland, S. Stafstrons, W. R. Salaneck, S. C. Graham, R. H. Friend, P. L. Burns and A. B. Holmes, *Synth. Met.*, 1993, **55–57**, 4320.
20 R. Stumpf and M. Scheffler, *Comput. Phys. Commun.*, 1994, **79**, 447.
21 G. Brocks, *J. Chem. Phys.*, 1996, **100**, 17327.
22 U. Salzner, J. B. Lagowski, P. G. Pickup and R. A. Poirier, *J. Comput. Chem.*, 1997, **18**, 1943.
23 S. Y. Hong, D. Y. Kim, C. Y. Kim and R. Hoffmann, *Macromolecules*, 2001, **34**, 6474.
24 S. Y. Hong, *Chem. Mater.*, 2000, **12**, 495.
25 S. Y. Hong and K. W. Lee, *Chem. Mater.*, 2000, **12**, 155.
26 Y. S. Lee, M. Kertesz and R. L. Eisenbaumer, *Chem. Mater.*, 1990, **2**, 526.
27 S. Y. Hong and D. S. Marynick, *Macromolecules*, 1992, **25**, 4652.
28 S. Y. Hong and J. M. Song, *J. Phys. Chem. B*, 1997, **101**, 10249.
29 U. Salzner, *J. Mol. Model.*, 2000, **6**, 195.
30 U. Salzner, C. J. Umrigar and X. Gonze, *Chem. Phys. Lett.*, 1998, **288**, 391.
31 R. Stowasser and R. Hoffmann, *J. Am. Chem. Soc.*, 1999, **111**, 6643.
32 D. J. Tozer, R. D. Amos, N. C. Handy, B. O. Roos and L. Serrano Andres, *Mol. Phys.*, 1999, **97**, 859.
33 O. Kwon and M. L. McKee, *J. Phys. Chem. B*, 2000, **104**, 1686.
34 P. Otto, *Int. J. Quantum Chem.*, 1994, **52**, 353.
35 P. Lahti, J. Obrzut and F. E. Karasz, *Macromolecules*, 1987, **20**, 2023.
36 J. L. Bredas, *Handbook of Conducting Polymers*, ed. T. A. Stotheim, Dekker, NY, 1986. p. 859.
37 G. Zotti, S. Martina, G. Wegner and A. D. Schluter, *Adv. Mater.*, 1992, **4**, 798.
38 M. J. S. Dewar, E. G. Zoebisch, E. F. Healy and J. J. P. Stewart, *J. Am. Chem. Soc.*, 1985, **107**, 3902.
39 A. D. Becke, *J. Chem. Phys.*, 1993, **98**, 5648.
40 W. M. F. Fabian, *J. Comput. Chem.*, 1988, **9**, 369.
41 S. Radhakrishnan, S. Parthasarathy, V. Subramaniyan and N. Somanathan, *J. Chem. Phys.*, 2005, **123**, 164905.
42 M. Mazzeo, V. Vitale, F. D. Sala, D. Pisignano, M. Anni, G. Barbarella, L. Favaretto, A. Zanelli, R. Cingolani and G. Gigli, *Adv. Mater.*, 2003, **15**, 2060.
43 J. Roncali, *J. Mater. Chem.*, 1999, **9**, 1875.
44 M. R. Anderson, M. Beggren, O. Inganas and G. Gustafsson, *Macromolecules*, 1995, **28**, 7525.
45 A. Bolognesi, W. Porzio, G. Bajo, G. Zannoni and L. Fannig, *Acta Polym.*, 1999, **50**, 151.
46 F. Meyers, A. J. Heeger and J. L. Bredas, *J. Chem. Phys.*, 1992, **97**, 2750.
47 G. J. Lee, S. K. Su, D. H. Kim, J. L. Lee and H. K. shim, *Synth. Met.*, 1995, **69**, 431.
48 S. Radhakrishnan, V. Subramanian, N. Somanathan, K. S. V. Srinivasan and T. Ramasami, *Mol. Cryst. Liq. Cryst.*, 2002, **390**, 113.
49 H. S. Woo, S. C. Graham, D. D. C. Bradley, R. H. Friend and A. B. Holmes, *Phys. Rev.*, 1992, **46**, 7379.
50 Y. Chen, R. Cai Bao and L. Yu, *Macromolecules*, 1993, **26**, 5281.
51 S. Hotta and K. Waragai, *Adv. Mater.*, 1993, **5**, 896.
52 S. Hotta and K. Waragai, *J. Phys. Chem.*, 1993, **97**, 7427.
53 J. Roncali, R. Garreau, A. Yassar, P. Marque, F. Garnier and M. Lemaire, *J. Phys. Chem.*, 1987, **91**, 6706.
54 O. Kwon and M. L. McKee, *J. Phys. Chem. A*, 2000, **104**, 7106.
55 *Electronic materials: The Oligomeric Approach*, ed. K. Mullen and G. Wegner, Wiley-VCH, Weinheim, 1998.
56 Z. Yuhong, W. Ming, X. Gouxing and Y. Weishen, *Chem. J. Internet*, 2000, **2**, 17.
57 M. Belletete, S. Beaupre, J. Bouchard, P. Blondin, M. Leclerc and G. Durocher, *J. Phys. Chem. B*, 2000, **104**, 9118.
58 W. M. F. Fabian, K. S. Niederreiter, G. Uray and W. Stadlbauer, *J. Mol. Struct.*, 1999, **477**, 209.
59 G. R. Hutchison, M. A. Ratner and T. J. Marks, *J. Phys. Chem. A*, 2002, **106**, 10596.
60 D. D. C. Bradley, M. Grell, A. Grice, A. R. Tajbakhsh, D. F. O'Brien and A. Bleyer, *Opt. Mater.*, 1998, **9**, 1.
61 M. J. Frisch, G. W. Trucks, H. B. Schlegel, G. E. Scuseria, M. A. Robb, J. R. Cheeseman, V. G. Zakrzewski, J. A. Montgomery, R. E. Stratmann, J. C. Brant, S. Dapprich, J. M. Millam, A. D. Daniels, K. N. Kudin, M. C. Strain, O. Farkas, J. Tomasi, V. Barone, M. Cossi, R. Cammi, B. Mennuci, C. Pomelli, C. Adamo, S. Clifford, J. Ochterski, G. A. Pattersson, P. Y. Ayala, Q. Cui, K. Morokuma, D. K. Malick, A. D. Rabuck, K. Raghavachari, J. B. Foresman, J. Cioslowski, J. V. Ortiz, B. B. Stefanov, G. Liu, A. Liashenko, P. Piskorz, I. Komaromi, R. Gomperts, R. L. Martin, D. J. Fox, T. Keith, M. A. Al-Laham, C. Y. Peng, A. Nanayakkara, C. Gonzalez, M. Challacombe, P. M. W. Gill, B. G. Johnson, W. Chen, M. W. Wong, J. L. Andres, M. Head-Gordon, E. S. Replogle and J. A. Pople, *GAUSSIAN 98W (Revision A.1)*, Gaussian, Inc., Pittsburgh, PA, 1998.
62 J. Ridley and M. Zerner, *Theor. Chim. Acta*, 1973, **32**, 111.